

Plastic strain is a mixture of avalanches and quasi-reversible deformations: Study of various sizes

Péter Szabó,* Péter Dusán Ispánovity, and István Groma

Department of Materials Physics, Eötvös University Budapest, H-1518 Budapest POB 32, Hungary

Size-dependence of plastic flow is studied by discrete dislocation dynamical simulation of systems with various numbers of interacting linear edge dislocations while the stress is slowly increased. Regions between avalanches in the individual stress curves as functions of the plastic strain were found nearly linear and reversible, where the plastic deformation obeys an effective equation of motion with a nearly linear force. For small plastic deformation, the means of the stress-strain curves are power law over two decades. Here and for somewhat larger plastic deformations, the mean stress-strain curves converge for larger sizes, while their variances shrink, both indicating the existence of a thermodynamical limit. The converging averages decrease with increasing size, in accordance with size-effects from experiments. For large plastic deformations, where steady flow sets in, thermodynamical limit was not realized in this model system.

PACS numbers: 61.72.Lk 81.40.Lm 83.50.-v

Introduction and overview: As known from research in the past decade, the stress-strain curve of micron-scale specimens contains random steps, where the plateaus mark avalanches, a behavior also observed in simulations.¹⁻⁶ Recently there has been a series of studies about the statistics of avalanches, and some on probabilistic properties of the yield stress,^{4,7,8} but the dependence of these features on the sample size was less investigated.^{7,9,10} The stair like stress-strain response caused by the dislocation avalanches become significant if the system size is in the order of $1\mu\text{m}$. Nevertheless, the size dependence of the plastic deformation is observed already at much larger system sizes. In most cases the smaller sample requires larger stress level to get the same deformation. The effect is traditionally modeled by large scale discrete dislocation dynamical (DDD)¹¹⁻¹⁴ simulations, phenomenological “nonlocal continuum theories” in which an appropriate gradient term is added to the stress-strain relation^{15,16}, or by continuum theory of dislocations¹⁷⁻²³. It is obvious, however, that a continuum theory is not applicable if the dislocation spacing is comparable to the system size.

In this paper the size-dependence of plastic deformations is studied by DDD simulation of systems with various numbers of interacting linear edge dislocations while the stress is slowly increased. Note that elastic deformations are not considered in this model, so strain and deformation are understood as purely plastic. Our main observations in this work are as follows. Between avalanches the stress grows close to linearly with the deformation. Tests of load cycles show that here the deformation is approximately reversible, so plasticity appears as a randomly alternating sequence of quasi-reversible deformations and avalanches. The linearity coefficient is random even for systems of the same size (number of dislocations N), with a sharpening distribution for larger N . In each realization, assuming an effective equation of motion for the deformation, we find a close-to-linear effective force, with a random spring constant. The full individual staircase-like stress-strain curves of the same N also

have a mean, which is a smooth function, different for different N 's. Up to a certain threshold deformation γ_{th} the mean stress-strain curve seems to converge for large N , while the variance goes to zero. So for large N essentially the same sharp stress-strain curve emerges for each realization, indicating the existence of a thermodynamic limit. This refines the finding of Tsekenis et al.⁹, where the natural scaling by \sqrt{N} let curves collapse even for smaller N . Within the region of thermodynamical limit $\gamma < \gamma_{\text{th}}$, for two decades in the strain, the mean stress-strain curve is a power law, with an exponent decreasing from 1 for small N to about 0.8 for large N . This is caused by the alternation of linear, quasi-reversible segments and plateaus of avalanches with random lengths in the stress-strain response function. Furthermore, for the model under study, there seems to be no thermodynamical limit for large deformations in the model under study.

Simulation method: Plastic deformation is mainly due to the motion of dislocations,²⁴ interacting via a long-range stress field. Here we study one of the simplest models of dislocation systems described as follows.^{1,25-28} Straight and parallel edge dislocations with parallel slip axes are considered, essentially a 2D cross section of a 3D system. Periodic boundary conditions are used on a square of side L , the slip axes are parallel to one edge of the square (the x axis), and for each realization dislocations are initially randomly placed with a uniform distribution. In the beginning each realization contains a fixed number N of dislocations, with equal number of positive and negative Burgers vectors $s(b, 0)$, where b is the lattice constant and $s = \pm 1$. Only dislocation glide is taken into account so the dislocations' vertical (y) coordinates are constant.

One positive dislocation induces the shear stress field

$$\tau_{\text{ind}}(\vec{r}) = bDx(x^2 - y^2)/r^4, \quad (1)$$

where $\vec{r} = (x, y)$ is the radius vector from that dislocation, $r = |\vec{r}|$, $D = \mu/[2\pi(1 - \nu)]$, with μ being the shear

modulus and ν the Poisson number. The i 'th dislocation is exposed to the shear stress field of all the others' $j \neq i$ and to the external field taken to be the uniform τ_{ext} , wherein it performs overdamped motion with drag coefficient B . Thus the equation of motion of the i 'th dislocation is^{6,29}

$$\dot{x}_i = B^{-1} b s_i \left[\sum_{\substack{j=1 \\ j \neq i}}^N s_j \tau_{\text{ind}}(\vec{r}_i - \vec{r}_j) + \tau_{\text{ext}} \right], \quad (2)$$

where the s_k is the sign of the k 'th dislocation and $\vec{r}_k = (x_k, y_k)$ its position. The plastic strain is calculated by $\gamma = b/L^2 \sum_i s_i \Delta x_i$, where Δx is the change in the x coordinate relative to the initial value. This equation is rendered periodic numerically by including sufficiently many mirror images of the j 'th dislocation. The resulting equation of motion is solved with 4.5th order Runge-Kutta method. Adaptive step size is used to better treat narrow dipoles. For very narrow dipoles would demand excessive computation time, we annihilate (different sign) or merge (same sign) dislocations if they are closer than $0.05 L/\sqrt{N}$. Whereas annihilation decreases the dislocation number, in order to avoid ambiguity, in the conversion formulas we use the original dislocation number N . Note that dislocations are not created in our model, corresponding to non-source-controlled plastic deformations. Throughout the paper simulations with $N = 32, 64, 128, 256, 512, 1024, 2048$ were considered with ensembles numbering $10^4, 3000, 2000, 800, 300, 100, 80$, respectively, and for the largest sizes our computational power allowed the scanning only of more restricted regions of simulated strain.

Equation (2) is represented in the computer by $B_{\text{cp}} = D_{\text{cp}} = b_{\text{cp}} = L_{\text{cp}} = 1$, yielding the density $\rho_{\text{cp}} = N/L_{\text{cp}}^2 = N$. The mapping to different sample sizes, while the physical dislocation density is kept constant, occurs by our introducing natural quantities $\gamma = \gamma_{\text{cp}}/\sqrt{N}$, $\tau = \tau_{\text{cp}}/\sqrt{N}$, $x = x_{\text{cp}}\sqrt{N}$, $t = t_{\text{cp}}N$, used throughout this paper.²⁶ Then physical quantities are obtained from the physical density ρ_{ph} as $L_{\text{ph}} = \sqrt{N/\rho_{\text{ph}}}$, $\gamma_{\text{ph}} = \gamma b_{\text{ph}}\sqrt{\rho_{\text{ph}}}$, $\tau_{\text{ph}} = \tau b_{\text{ph}} D_{\text{ph}}\sqrt{\rho_{\text{ph}}}$, $t_{\text{ph}} = t B_{\text{ph}}(b_{\text{ph}}^2 D_{\text{ph}} \rho_{\text{ph}})$. To give an example, if on the natural scale $\gamma = 0.35$ then for the generic physical variables $\rho_{\text{ph}} = 2 \cdot 10^{14} \text{m}^{-2}$ and $b_{\text{ph}} = 2 \text{\AA}$ we would obtain the physical deformation $\gamma_{\text{ph}} = 0.1\%$.

In the scenario presented here firstly we let the system relax without external stress to form the initial state with $\gamma = 0$. Then we apply quasi-static stress loading, i.e., we increase the external stress by a small rate, similar to what was applied earlier.^{7,9,30} Having experimented with various stress rates we finally chose $\dot{\tau}_{\text{ext}} = 5 \cdot 10^{-5}$. The stress is kept increasing so long as the mean absolute velocity of the dislocations remains under the threshold $5 \cdot 10^{-4}$. If that threshold is surpassed (this is our definition of an avalanche) then the external stress is kept constant until the mean absolute velocity drops again below the threshold. The end state is a steady flow, that

is, an infinite avalanche, because in the absence of dislocation creation no work hardening takes place for large deformations.

Individual stress-strain curves and effective motion between avalanches: We first show typical dislocation configurations for various plastic deformations γ along our scenario in Fig. 1. Firstly, dislocations relax in the ab-

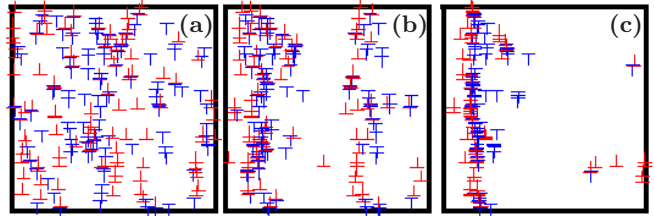


Figure 1. (Color online) Typical configuration at (a) relaxed state without external stress ($\gamma = 0$), (b) relaxed in the presence of medium external stress ($\gamma \approx 1$), (c) with external stress just below the steady flow ($\gamma \approx 1000$). The \perp (red) and the \top (blue) denote the $s = +/ -$ signs, respectively.

sence of external stress, forming a random-looking configuration of numerous smaller clusters, see Fig. 1a. Due to the increasing external stress the deformation γ generically increases, while clusters grow mainly in the y direction (1b). Beyond some threshold steady flow emerges, marked usually by a single dipolar wall, spanning across the whole simulation area (1c), while one-or-two dislocations are circling quickly along their slip axes, in conformance to the periodic boundary conditions. Hence we must conclude that in the steady flow boundary effects are important, thus our model may not be realistic in this region, and so we concentrate our study to smaller deformations.

The plastic stress-strain curves $\tau_{\text{ext}}(\gamma)$ of individual realizations are like staircases, they exhibit a sequence of plateaus of constant stress corresponding to avalanches, in accordance with earlier results,^{1-5,7} see Fig. 2. A novel observation here, to our knowledge not noted earlier, is that between plateaus, where the stress increases, the $\tau_{\text{ext}}(\gamma)$ functions are nearly linear. For the sake of comparison we normalized each increasing segment to a function $g(x)$ starting and ending at the opposite corners of the unit square as

$$g(x) = \frac{\tau_{\text{ext}}(x(\gamma_1 - \gamma_0) + \gamma_0) - \tau_0}{\tau_1 - \tau_0}, \quad x \in [0, 1], \quad (3)$$

where γ_0 , γ_1 and τ_0 , τ_1 mark the borders of the chosen segment. Such normalized segments of individual runs with $\gamma < 0.2$ were separately averaged for fixed sizes N , and the resulting curves fall onto each other and form $\langle g(x) \rangle$ in the inset of Fig. 2. Here, also the standard deviation of the normalized segments is plotted, which is again nearly the same for various N 's. So the segments between avalanches on the stress-strain curves, normal-

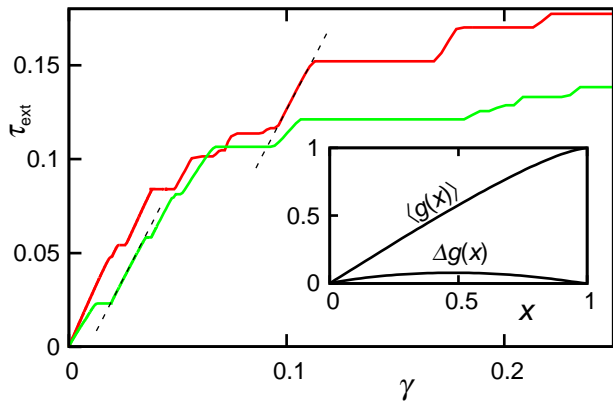


Figure 2. (Color online) Stress-strain curves $\tau_{\text{ext}}(\gamma)$ of two realizations of $N = 512$. Segments between plateaus are found to be nearly linear, dashed lines are guide to the eye. Inset: averages of increasing segments normalized as in Eq. (3) for fixed N 's all fall on the same curve, close to a linear function. The lower arc is the standard deviation, again nearly independent on N .

ized according to Eq. (3), follow on the average a universal, nearly linear form, with a universal variance.

In order to test properties of the close-to-linear segments, we have run a few loading cycles on individual realizations with various stress rates. In most of the cases, apart from a small, smooth, transient due to the finiteness of the stress rate, and from tiny avalanches, reversibility was found. Motivated by this “quasi-reversible” response, we surmise that deformations obey an effective equation of motion

$$\dot{\gamma}(t) \approx -F(\gamma(t) - \gamma_0) + \tau_{\text{ext}}(t) - \tau_0, \quad (4)$$

where (γ_0, τ_0) the endpoint of the last avalanche, where the system is assumed to be in equilibrium, and F is the effective restoring force, depending only on the increment $\gamma - \gamma_0$. Similarly as (3) associates $g(x)$ with the stress, we normalize the force $F(\gamma - \gamma_0)$ onto the unit square. Again, like the external stress in the inset of Fig. 2, the mean normalized force very weakly depends on N , and this universal function is astonishingly close to $g(x)$, which is the consequence of the low stress rate resulting $\dot{\gamma}(\gamma) \ll \tau_{\text{ext}}(\gamma)$. Thus even the force is very close to linear. We emphasize, that near equilibrium of a dislocation configuration, for small displacements, the elastic energy of course grows quadratically, so there the response should be linear. The remarkable feature in our case is that linearity holds way up to near the onset of the next avalanche. This instability is indeed marked by the slight curving of the universal function close to one in Fig. 2. Note that its slope there is not zero, whereas it would be zero in the case of a force-activated escape from a 1D potential, because of rare negative avalanches with $\dot{\gamma} < 0$.

In order to visualize the statistical nature of the quasi-reversible regions, in Fig. 3 we plot the cumulative prob-

ability distribution function $M(\lambda)$ of the steepness $\lambda = (\tau_1 - \tau_0)/(\gamma_1 - \gamma_0)$ for $\gamma \leq 0.2$ (chosen as a practical value). The curves visibly contract with increasing N , showing convergence to a finite mean. A nearly linear

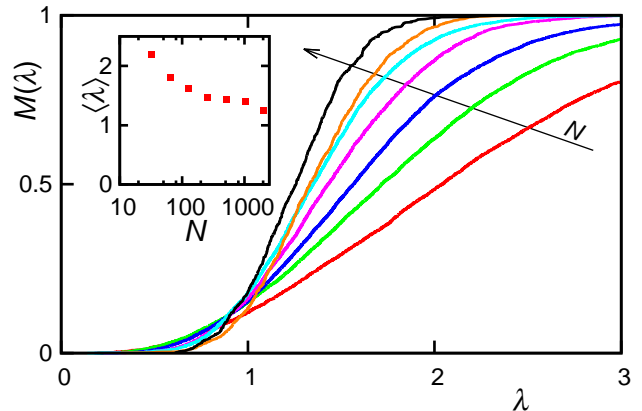


Figure 3. (Color online) Cumulative probability distribution function $M(\lambda, N)$ of the steepness λ of the quasi-linear segments with system sizes $N = 32, 64, \dots, 2048$ for $\gamma \leq 0.2$. The arrow points towards increasing N (colors distinguish sizes). Inset: the mean $\langle \lambda \rangle$ as functions of the system size N .

response here means that, due to the interaction of dislocations, an effective shear modulus arises. The latter can be interpreted as the plastic component of the total empirical shear modulus in real crystals. Note that in the present model elastic deformations are not included.

Mean stress as function of the strain: So far we concentrated on the quasi-reversible segments between avalanches, now we turn to the global statistical behavior of stress-strain curves. Firstly, we plot the average $\langle \tau_{\text{ext}} \rangle(\gamma, N)$ over ensembles with fixed N in Fig. 4. A main feature is the power law behavior over decades up to a strain approximately 0.05, (see inset), with exponent close to 1 for small sizes and decreasing with size to about 0.8. We can interpret this feature such that the nearly linear segments of the stress-strain curves are interrupted by the avalanche plateaus just in the way that an effective power function with a smaller-than-one exponent emerges. That is, avalanches soften the linearity of quasi-reversible segments and give rise statistically to a power law.

On physical scales, taking a lattice constant $b = 2\text{\AA}$, a dislocation density $\rho = 2 \cdot 10^{14}\text{m}^{-2}$, the $\gamma = 0.05$ corresponds to $\gamma_{\text{ph}} \approx 0.015\%$. It is important to note that this value is much smaller than the $\gamma_{\text{ph}} = 0.2\%$ threshold value customarily considered to be the yield strain in engineering practice. The fact that the power law arises way below the empirical yield value indicates the determining role of avalanches for much lower plastic strains than expected earlier. On the other hand, this is in a convincing agreement with fatigue experiments on single crystals that showed irreversibility already below the physical range of $\gamma_{\text{ph}} = 0.01\%$.³¹

Another important property seen in Fig. 4 is that

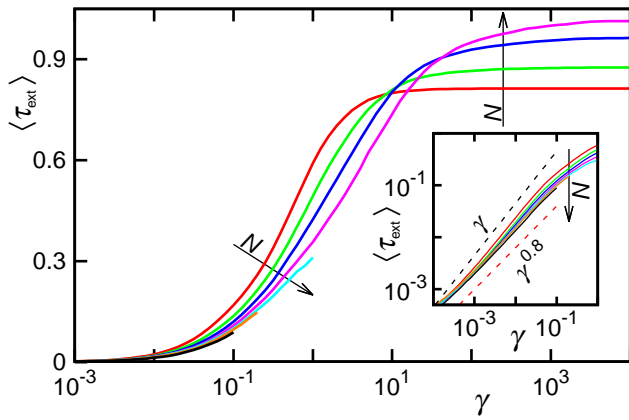


Figure 4. (Color online) Mean stress $\langle \tau_{\text{ext}} \rangle$ as a function of strain, for system sizes $N = 32, 64, \dots, 2048$, for large N only smaller γ 's were considered. Inset: log-log plot demonstrates the power law for $5 \cdot 10^{-4} \lesssim \gamma \lesssim 0.05$. The arrows point towards increasing N (colors distinguish sizes). The two dashed lines are guide to the eye.

for $\gamma \lesssim 1$ the stress-strain curves seem to converge for large N , a criterion for the existence of a thermodynamical limit. On the other hand, for large strains, the $N \rightarrow \infty$ tendency is inconclusive from our simulation, the stress values may even diverge. For intermediate strains $1 \lesssim \gamma \lesssim 100$ the convergent bundle of the curves switches order for the sizes we considered. Note that for fixed strains $\gamma \lesssim 1$ the stresses decrease with N . As discussed earlier in connection with physical units, increasing N here can mean increasing size with constant dislocation density. Therefore, larger stresses for smaller N 's as in Fig. 4 can be interpreted as a version of the property “smaller is harder”. We emphasize, however, that our model has periodic boundary conditions, thus pileups, commonly held responsible for this phenomenon,³² cannot develop. This tendency reverses for large strains, where the stress increases with N . In this region, however, where the configuration resembling a single wall forms, as seen in Fig. 1c, we do not suggest the model bears general relevance to real materials.

Standard deviation of the stress as a function of strain: Given the fact that the stress-strain response for macroscopic crystals with a fixed orientation is a well-defined, sharp curve, it is expected that the variance vanishes with increasing size. Accordingly, a decreasing variance was observed in micropillar experiments by Uchic *et al.*² To study this effect, we plotted in Fig. 5 the standard deviation $\Delta\tau_{\text{ext}}(\gamma, N)$ of the stress for ensembles with fixed N for different strains. In the region $\gamma \lesssim 1$, where the mean stress converged with N (see Fig. 4), the standard deviation decreases. We tested a power law convergence by plotting $\Delta\tau_{\text{ext}}(\gamma, N) \cdot N^{0.4}$ in the inset of Fig. 5, and indeed the collapse demonstrates that the deviation vanishes like $1/N^{0.4}$. Thus, recalling that we found a sharp limit for the average stress when $\gamma \lesssim 1$, we can conclude that in this region there is a thermodynamical limit. On

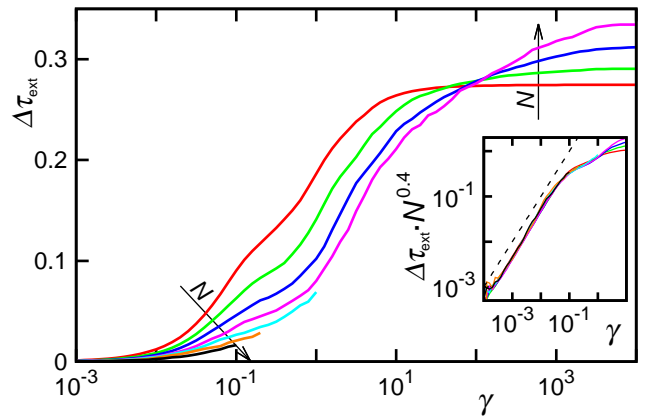


Figure 5. (Color online) Standard deviation $\Delta\tau_{\text{ext}}$ of the stress as function of the strain γ , for system sizes $N = 32, 64, \dots, 2048$, for large N only smaller γ 's were considered. The arrows point towards increasing N (colors distinguish sizes). Inset: log-log plot of $\Delta\tau_{\text{ext}} \cdot N^{0.4}$ shows collapse, the dashed line with power unity is a guide to the eye.

the contrary, for large strains Fig. 5 does not show convergence of the standard deviation, like there was no visible convergence of the mean in Fig. 4 either, so here thermodynamical limit is absent.

Conclusion and outlook: In this paper our aim was twofold. On the one hand, we uncovered quasi-reversible behavior with nearly linear response between avalanches in a 2D model of simulated dislocations. For large sizes, the effective plastic shear modulus appears to converge in average. As to the full stress-strain curves, the quasi-reversible segments conspire with the avalanche plateaus to yield on the average a power response curve. The second main question was about the thermodynamical limit, which is achieved by both a convergent mean and a vanishing variance of the stress for $\gamma \lesssim 1$. In this region we observed also the analog of the size-effect, as found in micropillars.² For largest strains thermodynamical limit is not reached and we do not consider our simulations as conclusive there.

Our study opens a series of questions. The results on the quasi-reversible behavior between avalanches call for more detailed investigations. The statistical properties of the finite-size behavior is best characterized by distribution functions, among which here we only described that of the local effective plastic shear modulus, characterizing quasi-reversible regions. The distribution of the stresses is of obvious interest, and at avalanches are expected to be related to extreme statistics. A longstanding problem in this area is the transition to steady flow, wherein the absence of a single critical point, rather critical behavior for all strains, has been shown before,²⁹ but a detailed study is still overdue. Carrying forth experiments on micropillars⁵ with various sizes and their comparison to the prediction from simulations would be of immediate interest.

Financial supports of the Hungarian Scientific Re-

search Fund (OTKA) under contract numbers K-105335 and PD-105256, and of the European Commission un-

der grant agreement No. CIG-321842 (StochPlast) are acknowledged.

-
- * pszabo@metal.elte.hu
- ¹ M.-C. Miguel, A. Vespignani, S. Zapperi, J. Weiss, and J.-R. Grasso, *Nature* **410**, 667 (2001)
 - ² M. D. Uchic, D. M. Dimiduk, J. N. Florando, and W. D. Nix, *Science* **305**, 986 (2004)
 - ³ M. D. Uchic, P. A. Shade, and D. M. Dimiduk, *Annu. Rev. Mater. Res.* **39**, 361 (2009)
 - ⁴ F. F. Csikor, C. Motz, D. Weygand, M. Zaiser, and S. Zapperi, *Science* **318**, 251 (2007)
 - ⁵ P. D. Ispánovity, A. Hegyi, I. Groma, G. Györgyi, K. Ratter, and D. Weygand, *Acta Mat.* **61**, 6234 (2013, Issue 16)
 - ⁶ P. D. Ispánovity, I. Groma, G. Györgyi, F. F. Csikor, and D. Weygand, *Phys. Rev. Lett.* **105**, 085503 (2010)
 - ⁷ V. Beato, M. Zaiser, and S. Zapperi, arXiv, 1106.3444v1(2011)
 - ⁸ M. LeBlanc, L. Angheluta, K. Dahmen, and N. Goldenfeld, *Phys. Rev. Lett.* **109**, 105702 (2012)
 - ⁹ G. Tsekenis, N. Goldenfeld, and K. A. Dahmen, *Phys. Rev. Lett.* **106**, 105501 (2011)
 - ¹⁰ P. M. Derlet and R. Maass, arXiv, 1401.3571(2014)
 - ¹¹ D. Balint, V. Deshpande, A. Needleman, and E. Van der Giessen, *Mod. Sim. Mat. Sci. Eng.* **14**, 409 (2006)
 - ¹² P. Guruprasad and A. Benzerga, *Phil. Mag.* **88**, 3585 (2008)
 - ¹³ D. Weygand, M. Pognant, P. Gumbsch, and O. Kraft, *Mat. Sci. Eng.* **483-84**, 188 (2008)
 - ¹⁴ A. A. Benzerga, *J. Mech. Phys. Solids* **57**, 1459 (2009)
 - ¹⁵ N. Fleck and J. Hutchinson, *J. Mech. Phys. Solids* **49**, 22452271 (2001)
 - ¹⁶ M. E. Gurtin, *J. Mech. Phys. Solids* **50**, 5 (2002)
 - ¹⁷ I. Groma, F. Csikor, and M. Zaiser, *Acta Mater.* **51**, 1271 (2003)
 - ¹⁸ I. Groma, G. Györgyi, and B. Kocsis, *Phys. Rev. Lett.* **96**, 165503 (2006)
 - ¹⁹ A. Acharya, A. Roy, and A. Sawant, *Scripta Mater.* **54**, 705 (2006)
 - ²⁰ J. Kratochvil and R. Sedlacek, *Phys. Rev. B* **77** (2008)
 - ²¹ S. D. Mesarovic, R. Baskaran, and A. Panchenko, *J. Mech. Phys. Solids* **58**, 311 (2010)
 - ²² S. Sandfeld, T. Hochrainer, M. Zaiser, and P. Gumbsch, *J. Mater. Res.* **26**, 623 (2011)
 - ²³ L. H. Poh, R. H. J. Peerlings, M. G. D. Geers, and S. Swaddiwudhipong, *J. Mech. Phys. Solids* **61**, 913 (2013)
 - ²⁴ F. R. Nabarro, *Theory of crystal dislocations*, Vol. 1 (Clarendon, 1967)
 - ²⁵ I. Groma and G. S. Pawley, *Phil. Mag. A* **67**, 1459 (1993)
 - ²⁶ F. F. Csikor, M. Zaiser, P. D. Ispánovity, and I. Groma, *Journal of Statistical Mechanics: Theory and Experiment* **2009**, P03036 (2009)
 - ²⁷ L. Laurson, M. C. Miguel, and M. J. Alava, *Phys. Rev. Lett.* **105**, 015501 (2010)
 - ²⁸ L. Laurson and M. Alava, *Phys. Rev. Lett.* **109**, 155504 (2012)
 - ²⁹ P. D. Ispánovity, I. Groma, G. Györgyi, P. Szabó, and W. Hoffelner, *Phys. Rev. Lett.* **107**, 085506 (2011)
 - ³⁰ P. M. Derlet and R. Maass, *Modelling Simul. Mater. Sci. Eng.* **21**, 035007 (2013)
 - ³¹ H. Mughrabi, *Metall. Mater. Trans. B* **40B**, 431 (2009)
 - ³² L. Kovács and L. Zsoldos, *Dislocations and plastic deformation* (Pergamon Press, 1973)